SCMNPs@Uridine/Zn: An efficient and reusable heterogeneous nanocatalyst for the rapid one-pot synthesis of tricyclic fused pyrazolopyranopyrimidine and 3-methyl carboxylate substituted pyrano[2,3-*c*]pyrazole derivatives under solvent-free conditions

Jia Wei[1]*, Wenjun Gui[1], Yanjun Cui[1], Zhifang Zhang[1], Qahtan A. Yousif[2]

[1]*Gansu Agricultural University, Institute of Agricultural Resources Chemistry and Application, College of Science, Gansu Province, 730000, China*
[2]*University of Al-Qadisiyah, College of Science, Department of Chemistry, Republic of Iraq*
**Corresponding author: e-mail: 1903908425@qq.com*

SCMNPs@Uridine/Zn is utilized as an environmental-friendly and efficient heterogeneous nanocatalyst for two one-pot four-component condensation reactions, containing hydrazine hydrate, arylaldehyde, ethyl acetoacetate, and barbituric acid to yield tricyclic fused pyrazolopyranopyrimidine derivatives (5a-q), and hydrazine hydrate, arylaldehyde, malononitrile, and dimethyl acetylenedicarboxylate/diethyl acetylenedicarboxylate to yield 3-methyl carboxylate substituted pyrano[2,3-*c*]pyrazole derivatives (8a-y) under solvent-free conditions with high to excellent yields. The main advantages of this process are easy work-up, short reaction times, no chromatographic purifications, and recyclability of the catalyst for a minimum of six runs without any significant decrease in yields of the products. Also, the prepared catalyst SCMNPs@Uridine/Zn was synthesized and fully characterized by various techniques including Fourier transform infrared spectroscopy (FT-IR), energy dispersive X-ray (EDX), thermogravimetric analysis (TGA), X-ray diffraction (XRD), vibrating sample magnetometer (VSM) and Raman spectroscopy.

Keywords: nanocatalyst, synthesis of tricyclic, carboxylate, efficient heterogeneous

INTRODUCTION

Catalyst plays a significant role in the industry as it can supply the highest yield of the desired product in the reduced time and temperature. A lot of systematic information about the catalytic properties has been established and accumulated from the literature. One of the most important information obtained relates to the limitations of catalytic reaction to separation and distribution[1–3]. Functionalization of the heterogeneous magnetic nanoparticles (MNPs) due to their unique features such as biocompatibility, simple modification, large surface area to volume ratios, and non-toxicity as the bridge with homogenous catalysts can also provide benefits of them including high activity and selectivity[4]. In addition to the above-mentioned features, easy separation from the reaction medium and reused of MNPs by an external magnetic field due to their paramagnetic nature make them the useful catalyst for sustainable and green chemistry. In order to protect the MNPs surface from oxidation and agglomeration due to the strong dipole-dipole attraction, and increase the dispersibility, efficiency, and colloidal stability of this type of magnetic nanoparticles, their surface has to protect by an organic (surfactants, polymers) or inorganic (carbon, silica, calcium hydroxyapatite) materials[5–10].

Pyrano[2,3-*c*]pyrazoles as privileged heterocyclic scaffolds are important biological compounds, due to their unique features such as insecticidal[11], bactericidal[12], molluscicidal[13–14], fungicidal[15], analgestic[16], and anti-inflammatory activities[17], and act as anti-tumor and anti-cancer[18] agents. The first strategy for the synthesis of pyrano[2,3-*c*]pyrazole derivatives were achieved through a two-component condensation of substituted pyrazol-5-ones and tetracyanoethylene[19]. However, these heterocyclic compounds have been achieved through a four-component reaction using hydrazine hydrate, dimethyl acetylenedicarboxylate, malononitrile, and aromatic aldehydes[20–21] Variety of catalysts, such as *L*-Proline[22], γ-alumina[23], glycine[24], piperidine[20], and imidazole[25] were reported for the preparation of pyrano[2,3-*c*] pyrazole derivatives but some of these strategies have disadvantages, including use of hazardous solvent, non-reusable catalysts, and long reaction times.

Pyrazolopyranopyrimidine and molecules containing this considerable unit represent a variety of pharmaceutical and biological activities, such as hypoglycemic[26], antidepressant[27], hypotensive[28], hepatoprotective[29], antitumor[30], antibronchitic[31], and antimicrobial[32]. The classical strategy for the synthesis of pyrazolopyranopyrimidine is the one-pot four component condensation of hydrazine hydrate, aldehyde, ethylacetoacetate, barbituric acid using base catalysts. During the last decade, novel procedures toward the synthesis of pyrazolopyranopyrimidine have been reported in the literature with a variety of catalysts, such as DABCO[33], OMWCNTs[34], TiO$_2$ NWs[35], [BNPs-Caff]HSO$_4$[36], Oleic acid[37], and Meglumine[38]. Most of these strategies suffer from disadvantages, such as requiring hazardous organic solvents, formation of by-product, large concentration of the catalyst, long reaction times, and difficulty in separation of the catalyst from the reaction solution. Therefore, the efforts for improving the reaction conditions for the preparation of pyrazolopyranopyrimidines using effective and reusable heterogeneous catalysts in the absence of solvent is a real challenge for synthetic chemists.

Experimental

All the pure chemicals were purchased from Fluka and Merck chemical companies. Fourier transform infrared (FT-IR) spectra were achieved on a PerkinElmer PXI instrument in KBr wafers. Scanning electron microscopy (SEM) studies performed using an SEM-LEO 1430VP

scanning electron microscope. Magnetic susceptibility measurements were performed with a PPMS 6000 vibrating sample magnetometer (VSM) at the magnetic field range of -10000 Oe to 10000 Oe at room temperature. The X-ray diffraction (XRD) studies were accomplished with a Siemens D-500 X-ray diffractometer (Munich, Germany). Thermogravimetric analysis (TGA) was carried out on a TGA thermoanalyzer (PerkinElmer) instrument. Elemental analysis was conducted using a Carlo-Erba EA1110CNNO-S. Raman analysis was conducted using a Witec Alpha 300 confocal Raman imaging microscope.

CATALYST SYNTHESIS

Preparation of Fe_3O_4 magnetic nanoparticles (MNPs)

Magnetic nanoparticles of Fe_3O_4 were achieved by an improved chemical co-precipitation procedure. Firstly, 7.3 g of $FeCl_3 \cdot 6H_2O$ and 3.2 g of $FeCl_2 \cdot 4H_2O$ salts were poured into a 250 mL flask reaction and dissolved in 150 mL of deionized water. Subsequently, 40 mL of ammonia solution was added dropwise into the reaction flask with vigorous stirring under a continuous flow of nitrogen gas at 70^oC for 50 min. Then the reaction solution was stirred and heated for another 1 h. The black precipitate MNPs was isolated by an appropriate magnetic field and rinsed with an equal mixture of deionized water and ethanol several times and then dried under vacuum at 60^oC.

Preparation of Magnetite/Silica (SCMNPs) Core-Shell Nanoparticles

The SCMNPs core-shell structures were obtained by modifying the Stöber strategy. At the beginning, 1 g of freshly prepared MNPs were poured into a 100 mL flask reaction, and then 7 ml of distilled water, 40 mL of ethanol and 4.0 mL of aqueous ammonia solution (25 wt%) was added to the reaction flask. In the following, the reaction mixture was sonicated for 35 min at room temperature. After this period of time, 0.5 mL of tetraethylorthosilicate (TEOS) was added dropwise into the reaction flask and sonicated for another 20 min. The reaction solution was stirred for 4h at room temperature. The resultant was extracted by an external magnetic field and washed with an equal mixture of deionized water and ethanol three times, and then dried under vacuum for 8 h.

Preparation of SCMNPs bonded 3-chloropropyl-triethoxysilane (SCMNPs@Pc)

1g of the prepared SCMNPs was dispersed in 100 mL of dry toluene and mixed with 2 mL of 3-chloropropyl-triethoxysilane (CPTCSi), and the resultant mixture was refluxed for 24 h under a continuous flow of nitrogen gas. The precipitates of core-shell SCMNPs@Pc nanoparticles were separated using a powerful external magnet and washed with 3×10 mL of distilled water to eliminate the unreacted organic groups and next dried in a vacuum oven for 15 h.

Preparation of SCMNPs@Pc/TSC

1 g of core-shell SCMNPs@Pc nanoparticles was poured in 50 mL ethanol and dispersed with the aid of ultrasonication for 30 min. Next, 5 mL of thiosemicarbazide (TSC) was added into the reaction solution, and the contents of the reaction vessel were refluxed for 24 h under the nitrogen atmosphere. After that, the precipitates were isolated from the solution by a powerful magnet and then rinsed three times with an equal mixture of ethanol and distilled water. Finally, the resulted product (SCMNPs@Pc/TSC) was dried in a vacuum oven for 12 h.

Preparation of SCMNPs@Uridine

1 g of the prepared SCMNPs@Pc/TSC was dispersed in 100 mL of an equal mixture of ethanol and water and mixed with 0.9 g of uridine. The resultant mixture was stirred at 90^oC for 10 h. The resultant solid (SCMNPs@Uridine) was isolated using an external magnet and rinsed three times to remove the unreacted organic groups and dried in a vacuum oven for 15 h.

Preparation of SCMNPs@Uridine/Zn

1 g of SCMNPs@Uridine and 0.2 g of $ZnCl_2$ was added in 30 mL of acetonitrile and then was stirred for 24 h under nitrogen atmosphere. After the specified time, the precipitate of SCMNPs@Uridine/Zn formed was isolated by magnetic decantation, rinsed three times with 3×10 mL of ethanol to eliminate unreacted metal precursors. Last of all, the resultant dried under vacuum oven for 15 h to achieve the pure product. All stages of the SCMNPs@Uridine/Zn synthesis are shown in Scheme 1.
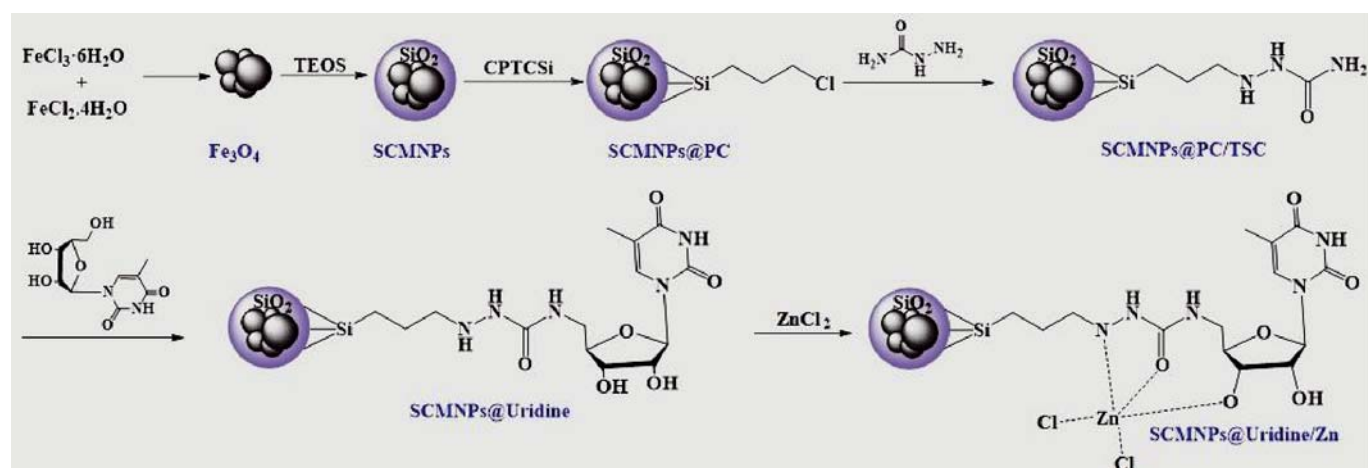
Scheme 1. All stages of the SCMNPs@Uridine/Zn synthesis

RESULTS AND DISCUSSIONS

FTIR analysis of SCMNPs@Uridine/Zn

The FT-IR spectra of MNPs, SCMNPs, SCMNPs@Pc, SCMNPs@Pc/TSC and SCMNPs@Uridine, SCMNPs@Uridine/Zn were shown in Fig. 1. In the FTIR spectrum of the MNPs, the peak at 593 and 459 cm^{-1} were attributed to the characteristic Fe-O-Fe vibration of the magnetite phase, and the peak at 3356 cm^{-1} was attributed to the characteristic O-H stretching vibration. The absorption peaks of the SCMNPs at 1095 and 951 cm^{-1} are connected to the stretching vibration of Si-O-Si and Si-OH groups, respectively. The absorption peaks of the aliphatic group in the SCMNPs@Pc at 2983 cm^{-1} can be ascribed to stretching vibrations of C-H bond. The spectra of SCMNPs@Pc/TSC showed the characteristic bending vibration of N-H, stretching vibration of C=S, and stretching vibration of N-H at 1476, 1305, and 3312 cm^{-1}, respectively. As can be seen from the spectra of SCMNPs@Uridine/Zn, the functionalization of SCMNPs@Pc/TSC with uridine can be confirmed by bands at 1576 and 1411 cm^{-1} resulting from the C=C group.
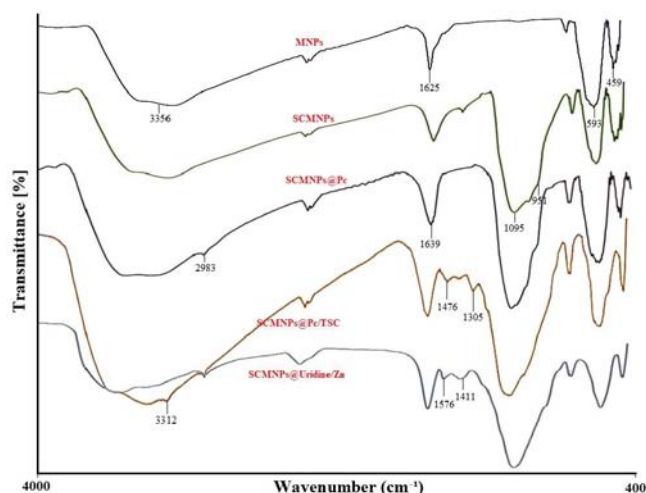
Figure 1. The FTIR spectra of MNPs, SCMNPs, SCMNPs@Pc, SCMNPs@Pc/TSC and SCMNPs@Uridine/Zn

VSM analysis of SCMNPs@Uridine/Zn

The magnetic features of the MNPs, SCMNPs, and SCMNPs@Uridine/Zn were appointed at room temperature by using a vibrating sample magnetometer (VSM) (Fig. 2). The saturation magnetizations (Ms) for MNPs, SCMNPs, and SCMNPs@Uridine/Zn were discovered to be 61.42, 40.15, and 33.59 emu/g, respectively. Compared with the MNPs, a clear decrease in the saturation magnetization of the SCMNPs confirms the formation influence of the silica layers on the surface of the magnetic nanoparticles. Furthermore, a decrease in the saturation magnetization of the SCMNPs@Uridine/Zn, confirms functionalization of the MNPs with the organic moieties

Raman analysis of SCMNPs@Uridine/Zn

In order to discern both phases of iron oxides, the Raman microscope was applied to collect the spectra of MNPs, SCMNPs, and SCMNPs@Uridine/Zn at several regions (Fig. 3). In all of the samples, the main band around 654 cm^{-1} is observed. This band can be attributed to the intrinsic stretching vibrations of oxygen atoms
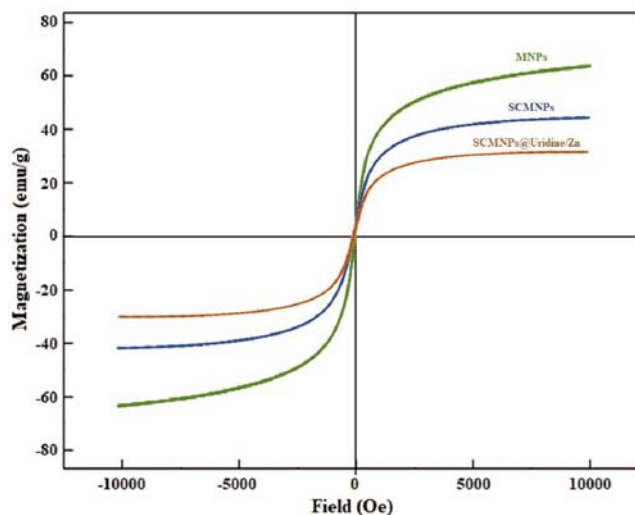

Figure 2. The magnetization curves of the MNPs, SCMNPs, and SCMNPs@Uridine/Zn
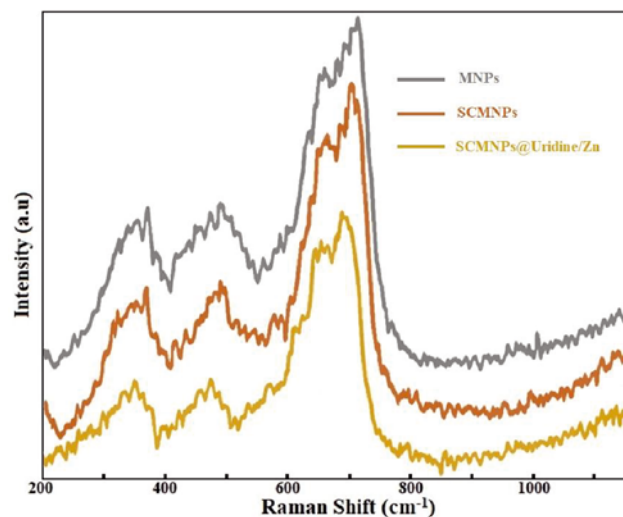

Figure 3. Raman spectra of the MNPs, SCMNPs, and SCMNPs@Uridine/Zn

along Fe-O bonds of magnetic Fe$_3$O$_4$ nanoparticles. In addition, the bands at 345 (E$_g$), 478 (T$_{2g}$), and 695 (A$_{1g}$) cm^{-1} related to the maghemite can be seen. These results confirmed that the magnetic nanocatalyst is successfully composed of the maghemite and magnetite phases of iron oxide.

XRD analysis of SCMNPs@Uridine/Zn

The structure of MNPs, SCMNPs, and SCMNPs@Uridine/Zn were characterized by X-ray diffraction (XRD) spectroscopy (Fig. 4). XRD analysis of the MNPs exhibited close patterns to the patterns of spinel ferrites explained in the literature (JCPDS NO. 88-0315). Also, the same peaks were achieved for the SCMNPs, and SCMNPs@Uridine/Zn XRD patterns compared to the MNPs, indicating retention of the spinel phase of magnetic iron oxide nanoparticles during the silica-coating process.

TGA analysis of SCMNPs@Uridine/Zn

The thermal stability of MNPs, SCMNPs, SCMNPs@Pc, SCMNPs@Pc/TSC, and SCMNPs@Uridine/Zn were investigated using TGA. The results of these analyses
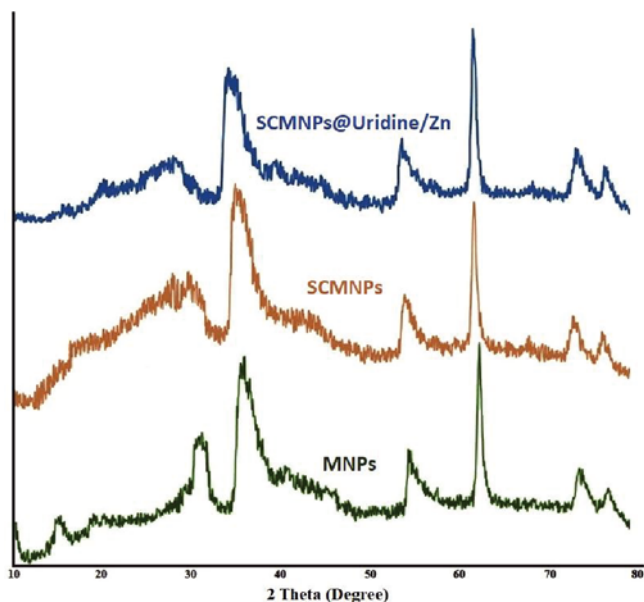
Figure 4. XRD pattern of MNPs, SCMNPs, and SCMNPs@ Uridine/Zn

are shown in Fig. 5. In all of the samples, initial weight loss was achieved up to 150°C due to the loss of the physisorbed and chemisorbed hydroxyl groups and solvents on the support and silica layers. In the case of SCMNPs@Pc, a weight loss appears below 320°C due to the decomposition of the attached organic molecule of 3-chloropropyltriethoxysilane on the Fe_3O_4 MNPs surface. Moreover, the TGA curves of SCMNPs@Pc/TSC and SCMNPs@Uridine/Zn, several weight loss in the range from 200 to 600°C, resulting from the decomposition of the covalently attached organic moieties
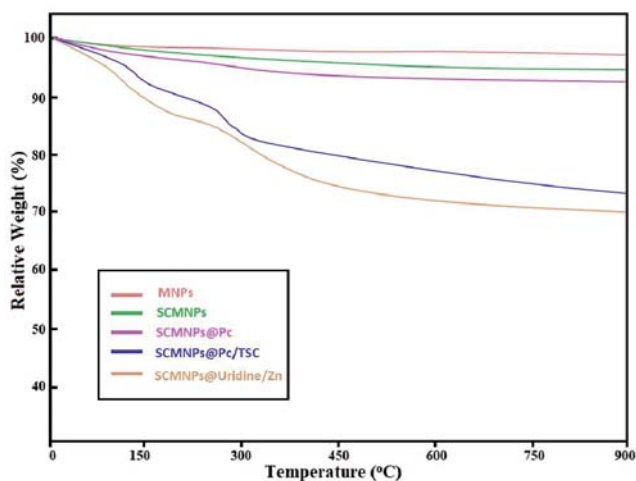
Figure 5. TGA curves of MNPs, SCMNPs, SCMNPs@Pc, SCMNPs@Pc/TSC and SCMNPs@Uridine/Zn

EDX analysis of SCMNPs@Uridine/Zn

The EDX result of SCMNPs@Uridine/Zn sample is depicted in Fig. 6, indicating the presence of Fe, Si, N, O, C, S and Zn in the prepared catalyst. The existence of C, O, N, and S elements demonstrates the successful loading of uridine onto the surface of the silica-coated magnetic nanoparticles. Moreover, the presence of Zn signals indicates the coordination of Zn with the organic molecules on the surface of the material. According to these results, it can be expected that SCMNPs@Uridine/ Zn catalyst had been successfully prepared.
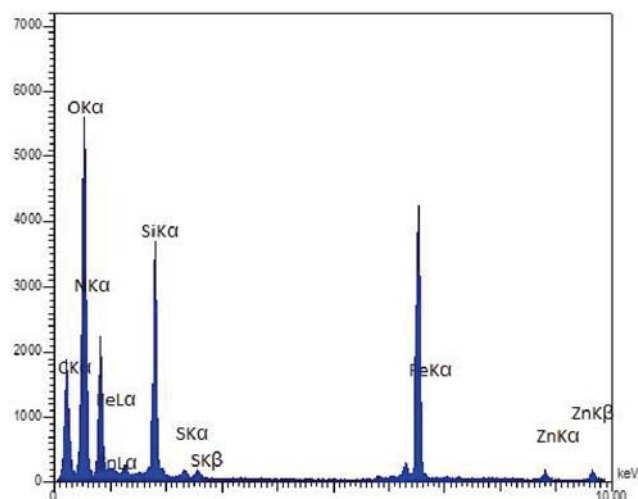

Figure 6. EDX spectrum of SCMNPs@Uridine/Zn

In this research, we reported our outcomes for the rapid and efficient synthesis of tricyclic fused pyrazolopyranopyrimidine and 3-methyl carboxylate substituted pyrano[2,3-*c*]pyrazole derivatives using SCMNPs@Uridine/ Zn as an effective heterogeneous magnetic nanocatalyst under solvent-free conditions (Scheme 2).
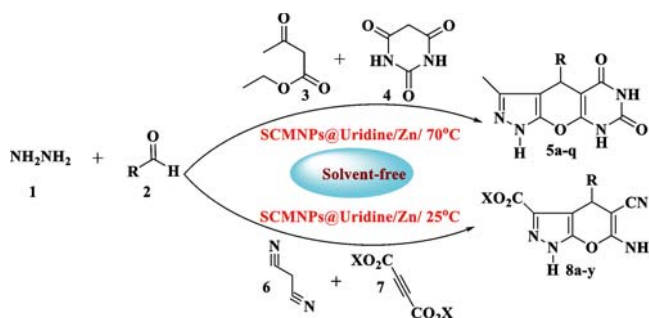
Scheme 2. Synthesis of tricyclic fused pyrazolopyranopyrimidine and 3-methyl carboxylate substituted pyrano[2,3-*c*]pyrazole derivatives using SCMNPs@Uridine/Zn

For our initial investigation and in order to optimize the reaction conditions, the reaction of hydrazine hydrate (1 mmol), benzaldehyde (1 mmol), ethyl acetoacetate (1 mmol), and barbituric acid (1 mmol) was accomplished using different amounts of catalyst with numerous solvents in the absence and presence of temperature. The results are summarized in Table 1. In the beginning, solvents such as H_2O, EtOH, MeOH, DMF, $CHCl_3$, CH_3CN, THF, and solvent-free conditions were applied separately for the synthesis of tricyclic fused pyrazolopyranopyrimidine 5a (Table 1, Entries 1–8). As illustrated in this table, water was the best choice for model reaction, especially as a green solvent compared with the other organic solvents (Table 1, Entry 1). In the following study on solvents, synthesis of the desired product 5a was carried out without solvent (Table 1, Entry 8). The results were encouraging due to shorter reaction time and higher yield. During the optimization of the reaction condition, various temperatures (25, 60, 70, 80, 90, and 100°C) were also screened to test their efficiency, and the results are tabulated in this table (Table 1, Entries 8–13). The highest reaction activity was achieved in the system at 70°C under solvent-free

conditions in comparison to other temperatures under similar reaction conditions (Table 1, Entry 8). Increasing the reaction temperature did not improve the yield of 5a (Table 1, Entries 11–13). At room temperature and temperatures lower than 70°C, we could not isolate the excellent yield of our desired four-component product. In order to clarify the need for the SCMNPs@Uridine/Zn nanocatalyst, various amounts of the catalyst, such as 15, 20, and 25 mg, were used to find the optimum reaction media (Table 1, Entries 8 and 14–15). As is evident, by increasing the amount of catalyst (20 to 25 mg), the yield of the product was not improved (Table 1, Entry 14) and also by decreasing it to 15 mg, the product quantity was changed from excellent to good yield (Table 1, Entry 15). In the final section of the study, in order to determine the ability of SCMNPs@Uridine/Zn in preparation of tricyclic fused pyrazolopyranopyrimidine derivatives, the efficiency of SCMNPs@Uridine/Zn for the reaction of hydrazine hydrate, aldehyde, ethylacetoacetate, and barbituric acid was compared with previously reported catalysts in the literature (Table 1, Entries 16–21). Thus, this procedure with SCMNPs@Uridine/Zn as the novel heterogeneous nanocatalyst seems superior to other recently reported synthetic methods.

Having optimized reaction conditions at hand, a highly efficient one-pot four-component synthesis of tricyclic fused pyrazolopyranopyrimidine derivatives has also been developed applying the same methodology (Table 2). To determine the limitation of the reaction, the reaction of barbituric acid with various aromatic aldehydes was performed according to the general optimized experimental procedure. The corresponding products are tabulated in this table. The yields of most products are higher than 89%. Thus, the aldehydes bearing electron-withdrawing groups and also electron-donating substituents (2a–q) gave the corresponding products with hydrazine hydrate (1), ethyl acetoacetate (3), and barbituric acid (4) under the optimized conditions (Table 2, Entries 1–16). As shown, in the presence of SCMNPs@Uridine/Zn as a catalyst, excellent yields of the product were achieved in shorter reaction times under solvent-free conditions.
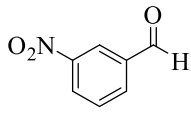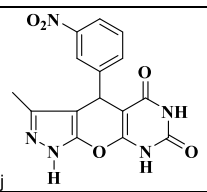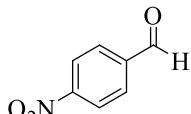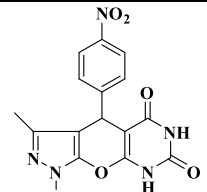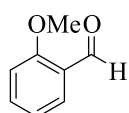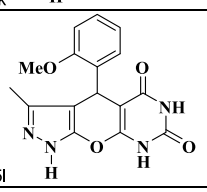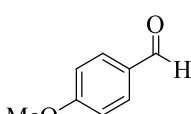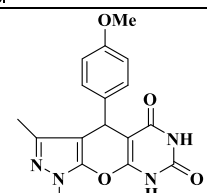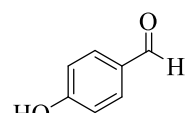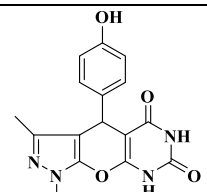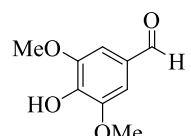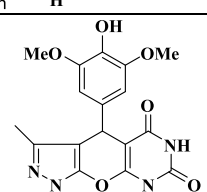
To optimize the reaction conditions, condensation of hydrazine hydrate (1 mmol), 4-nitrobenzaldehyde (1 mmol), malononitrile (1 mmol), and dimethyl acetylenedicarboxylate (7a) /diethyl acetylenedicarboxylate (7b) (1 mmol) was selected as a model reaction (Table 3). The above four-component reaction was performed at different temperatures and solvents in the various am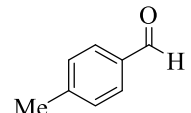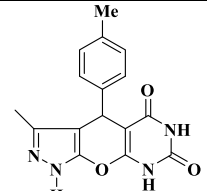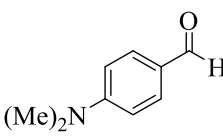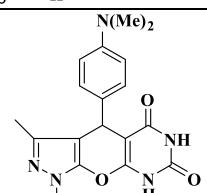ounts of the catalyst to establish the real efficacy of the SCMNPs@Uridine/Zn catalyst. To compare the effects of solvent on the reaction, various solvents such as H_2O, EtOH, H_2O/EtOH, CH_2Cl_2, CH_3CN, and under solvent-free conditions were utilized (Table 3, Entries 1–6). Among the solvents mentioned above, H_2O was found to be the best one, generating the high yield of the product (Table 3, Entry 1). Moreover, when the reaction was performed under solvent-free conditions, the target product was obtained with excellent yield and short reaction time (Table 3, Entry 6). Moreover, the model reaction was tested in the presence of various molar ratios of SCMNPs@Uridine/Zn at 25°C under solvent-free conditions (Table 3, Entries 6, and 13–14). These entries indicate that an excellent yield and a short reaction time was achieved when the reaction was performed in the presence of 15 mg of the catalyst in the absence of solvent; under

Table 1. Optimization of reaction condition using different conditions[a]
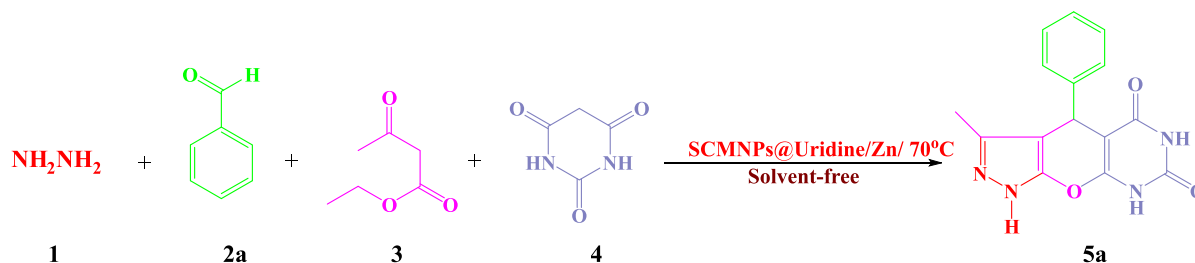
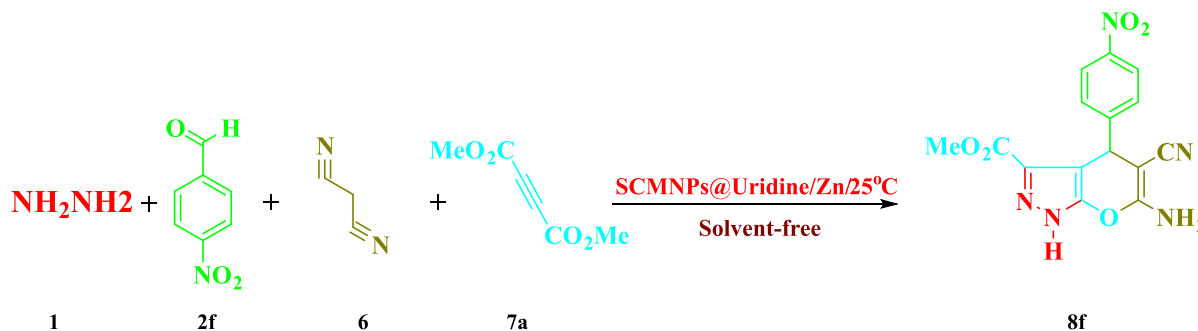| Entry	Solvent	Catalyst [mg]	Temp.	Time [min]	Yield [%][b]	Ref
1	H_2O	SCMNPs@Uridine/Zn /20	Reflux	30	95	This work
2	EtOH	SCMNPs@Uridine/Zn /20	Reflux	60	56	This work
3	MeOH	SCMNPs@Uridine/Zn /20	Reflux	60	79	This work
4	DMF	SCMNPs@Uridine/Zn /20	Reflux	100	35	This work
5	$CHCl_3$	SCMNPs@Uridine/Zn /20	Reflux	80	81	This work
6	CH_3CN	SCMNPs@Uridine/Zn /20	Reflux	60	88	This work
7	THF	SCMNPs@Uridine/Zn /20	Reflux	100	29	This work
8	Solvent- free	SCMNPs@Uridine/Zn /20	70°C	15	97	This work
9	Solvent- free	SCMNPs@Uridine/Zn /20	25°C	80	32	This work
10	Solvent- free	SCMNPs@Uridine/Zn /20	60°C	20	92	This work
11	Solvent- free	SCMNPs@Uridine/Zn /20	80°C	20	95	This work
12	Solvent- free	SCMNPs@Uridine/Zn /20	90°C	20	93	This work
13	Solvent- free	SCMNPs@Uridine/Zn /20	100°C	20	91	This work
14	Solvent- free	SCMNPs@Uridine/Zn /25	70°C	15	97	This work
15	Solvent- free	SCMNPs@Uridine/Zn /15	70°C	35	89	This work
16	H_2O	DABCO	Reflux	20	99	33
17	EtOH/ H_2O	OMWCNTs	Reflux	70	94	34
18	EtOH/ H_2O	TiO_2 NWs	Reflux	60	95	35
19	H_2O	[BNPs-Caff]HSO_4	50°C	40	95	36
20	H_2O	Oleic acid	Reflux	12	82	37
21	H_2O	Meglumine	r.t.	15	90	38

[a] Reaction conditions: hydrazine hydrate (1 mmol), benzaldehyde (1 mmol), ethyl acetoacetate (1 mmol) barbituric acid (1 mmol),and the required amounts of the catalysts. [b] The yields refer to the isolated product.

Table 2. Synthesis of tricyclic fused pyrazolopyranopyrimidine derivatives[a]

Entry	RCHO (2)	Product	Yield[%][b]/ Time [min]	M.P (Obsd)[(°C]	M.P (Lit)[°C]
1		5a	97/15	219–221	218–220[36]
2		5b	93/17	222–224	223–225[36]
7		5c	94/15	245–248	247–247[38]
3		5d	95/17	221–224	222–223[36]
4		5e	91/20	232–235	233–234[36]
5		5f	90/25	248–251	250–251[38]
6		5g	93/15	135–138	128–129[38]
7		5h	91/20	212–215	211–212[36]
8		5i	92/35	208–210	208–209[36]

9		5j	90/17	264–266	266–267[36]
10		5k	96/15	232–235	233–234[36]
11		5l	89/25	229–231	230–231[36]
12		5m	94/25	232–235	228–230[36]
13		5n	92/20	261–264	263–265[35]
14		5o	95/30	239–241	240–242[38]
15		5p	90/25	201–203	200–201[33]
16		5q	96/25	261–263	260–262[36]

[a] Reaction conditions: hydrazine hydrate (1 mmol), aldehyde (1 mmol), ethylacetoacetate (1 mmol), barbituric acid (1 mmol), and SCMNPs@Uridine/Zn (20 mg).

these conditions, the corresponding 3-methyl carboxylate substituted pyrano[2,3-*c*]pyrazole 8f was produced in 97% yield within 15 min (Table 3, Entry 6). Increasing the amount of the catalyst to 20 mg illustrated no substantial improvement in the yield of product (Table 3, Entry 13), whereas the yield diminished by decreasing the amount of catalyst to 10 mg (Table 3, Entry 14). Also, the effect of temperature on the transformation was examined, and the results obtained were summarized in Table 3. It is obvious that at 25ºC, a high yield of product was obtained (Table 3,

Entry 6). With an increase in the temperature from 40ºC to 90ºC, the product was achieved without any increase in the yield (Table 3, Entries 7–12). In order to show the efficiency of this procedure, we have compared our results from the synthesis of 3-methyl carboxylate substituted pyrano[2,3-*c*]pyrazoles using SCMNPs@Uridine/Zn as the catalyst with some of the previously reported methods (Table 3, Entries 15–20). As it is clear from these entries, the use of SCMNPs@Uridine/Zn leads to an improved protocol in

Table 3. Optimization of the three-component reaction of hydrazine hydrate, 4-nitrobenzaldehyde, malononitrile, and dimethyl acetylenedicarboxylate (7a)/diethyl acetylenedicarboxylate (7b) under various conditions[a]

Entry	Solvent	Catalyst [mg]	Temp.	Time [min]	Yield [%][b]	Ref
1	H_2O	SCMNPs@Uridine/Zn /15	Reflux	25	95	This work
2	EtOH	SCMNPs@Uridine/Zn /15	Reflux	25	83	This work
3	H_2O/EtOH	SCMNPs@Uridine/Zn /15	Reflux	25	87	This work
4	CH_2Cl_2	SCMNPs@Uridine/Zn /15	Reflux	45	71	This work
5	CH_3CN	SCMNPs@Uridine/Zn /15	Reflux	35	75	This work
6	Solvent- free	SCMNPs@Uridine/Zn /15	25°C	15	97	This work
7	Solvent- free	SCMNPs@Uridine/Zn /15	40°C	15	95	This work
8	Solvent- free	SCMNPs@Uridine/Zn /15	50°C	15	95	This work
9	Solvent- free	SCMNPs@Uridine/Zn /15	60°C	15	93	This work
10	Solvent- free	SCMNPs@Uridine/Zn /15	70°C	15	92	This work
11	Solvent- free	SCMNPs@Uridine/Zn /15	80°C	15	92	This work
12	Solvent- free	SCMNPs@Uridine/Zn /15	90°C	15	90	This work
13	Solvent- free	SCMNPs@Uridine/Zn /20	25°C	15	97	This work
14	Solvent- free	SCMNPs@Uridine/Zn /10	25°C	25	89	This work
15	H_2O	nao-ZnZr$_4$(PO$_4$)$_6$	25°C	30–42	83–93	39
16	H_2O	CeO$_2$ nanoparticles	25°C	25–39	82–91	40
17	H_2O	–	55–60°C	1.5–2.5	64–84	41
18	H_2O	ɤ-Alumina	Reflux	35–90	61–90	23[c]
19	H_2O	Ba(OH)$_2$	Reflux	60–120	81–93	42[c]
20	EtOH	Amberlyst A21	25°C	10–65	73–98	43[c]

[a] Reaction conditions: hydrazine hydrate (1 mmol), 4-nitrobenzaldehyde (1 mmol), malononitrile (1 mmol), dimethyl acetylenedicarboxylate (7a) (1 mmol) and 15 mg of the catalyst. [b] The yields refer to the isolated product. [c] Reaction conditions: hydrazine hydrate (1 mmol), aldehyde (1 mmol), malononitrile (1 mmol), diethyl acetylenedicarboxylate (1 mmol) (7b).

the product yields, reaction times, compatibility with the environment, and the amount of the catalyst.

After optimization of the reaction conditions, a wide range of structurally-diverse aldehydes (2) containing electron-withdrawing as well as electron-donating groups such as Cl, F, Br, NO$_2$, OCH$_3$, and OH in the ortho, meta, and para positions on the benzene ring were reacted with hydrazine hydrate (1), malononitrile (4), dimethyl acetyle-nedicarboxylate (7a)/diethyl acetylenedicarboxylate (7b), in the presence of SCMNPs@Uridine/Zn at 25°C to provide the corresponding products in high yields and short reaction times (Table 4, Entries 1–25).

On the basis of the above result, a plausible mechanism for the formation of tricyclic fused pyrazolopyranopyrimi-dine derivatives from hydrazine hydrate, aldehyde, ethyla-cetoacetate and barbituric acid was described in Scheme 3.
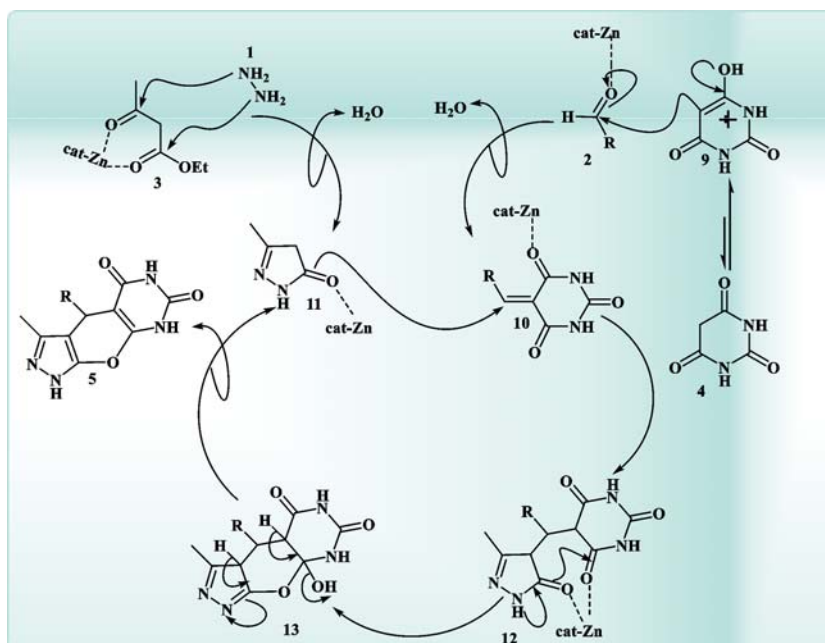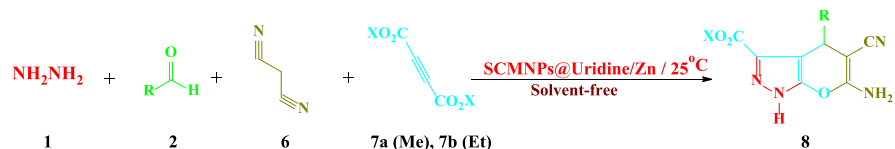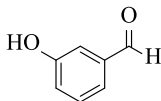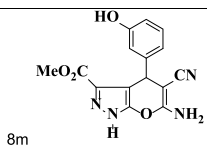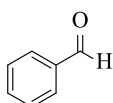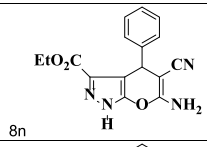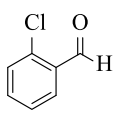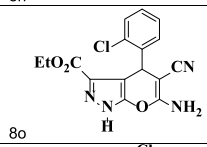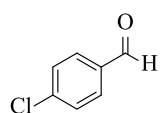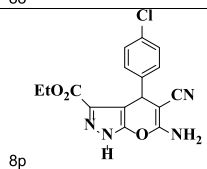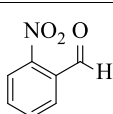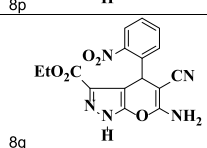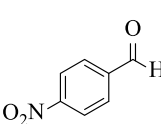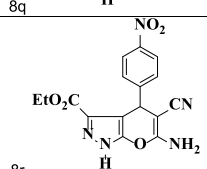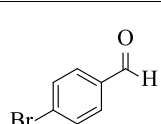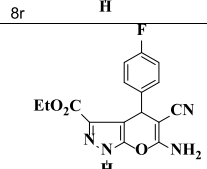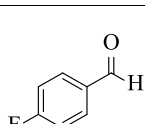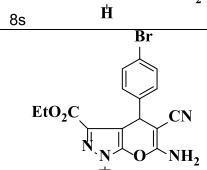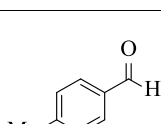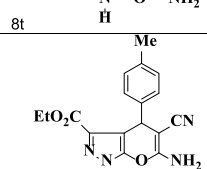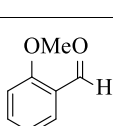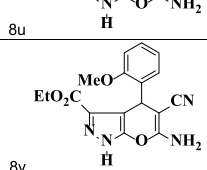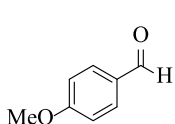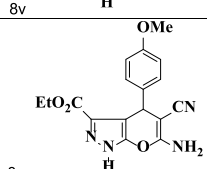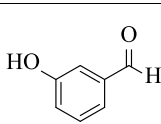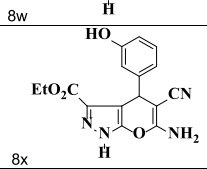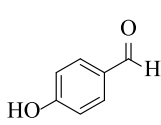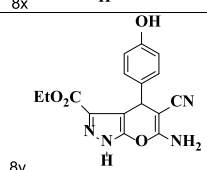

Scheme 3. Plausible mechanism for synthesis of tricyclic fused pyrazolopyranopyrimidine derivatives

Table 4. Synthesis of 3-methyl carboxylate substituted pyrano[2,3-*c*]pyrazoles by SCMNPs@Uridine/Zn catalyst[a]

Entry	RCHO (2)	Product	Yield[%][b]/Time [min]	M.P[Obsd][°C]	M.P [Lit][°C]
1		8a	90/15	230–233	231–232[41]
2		8b	92/15	249–251	248–250[39]
3		8c	93/17	249–251	247–248[41]
4		8d	95/17	229–231	230–232[41]
5		8e	94/17	235–238	236–237[41]
6		8f	97/15	243–245	244–245[41]
7		8g	93/17	238–240	239–240[41]
8		8h	94/15	241–243	242–244[39]
9		8i	93/20	210–212	212–214[41]
10		8j	94/25	207–209	208–210[41]
11		8k	93/17	239–241	238–240[39]
12		8l	90/20	240–242	239–241[39]

Entry	Aldehyde	Product		mp (°C)	mp (lit.)
13	HO–C₆H₄–CHO (3-hydroxybenzaldehyde)	8m (MeO₂C, CN, NH₂ pyrano-pyrazole, 3-hydroxyphenyl)	92/20	218–221	219–220[41]
14	benzaldehyde	8n (EtO₂C, phenyl)	92/20	209–211	208–210[44]
15	2-chlorobenzaldehyde	8o (EtO₂C, 2-chlorophenyl)	93/15	217–219	218–220[44]
16	4-chlorobenzaldehyde	8p (EtO₂C, 4-chlorophenyl)	97/10	235–237	236–238[44]
17	2-nitrobenzaldehyde	8q (EtO₂C, 2-nitrophenyl)	95/17	234–236	235–237[45]
18	4-nitrobenzaldehyde	8r (EtO₂C, 4-nitrophenyl)	96/10	208–210	210–212[44]
19	4-bromobenzaldehyde	8s (EtO₂C, 4-fluorophenyl)	95/15	223–226	225–227[45]
20	4-fluorobenzaldehyde	8t (EtO₂C, 4-bromophenyl)	95/10	223–225	224–226[44]
21	4-methylbenzaldehyde	8u (EtO₂C, 4-methylphenyl)	95/15	212–215	212–214[44]
22	2-methoxybenzaldehyde	8v (EtO₂C, 2-methoxyphenyl)	92/15	206–209	205–207[45]
23	4-methoxybenzaldehyde	8w (EtO₂C, 4-methoxyphenyl)	94/15	207–209	208–210[45]
24	3-hydroxybenzaldehyde	8x (EtO₂C, 3-hydroxyphenyl)	89/10	222–224	221–223[45]
25	4-hydroxybenzaldehyde	8y (EtO₂C, 4-hydroxyphenyl)	93/10	205–208	204–206[44]

[a] Reaction conditions: hydrazine hydrate (1 mmol), aldehyde (1 mmol), malononitrile (1 mmol), dimethyl acetylenedicarboxylate (7a)/ diethyl acetylenedicarboxylate (7b) (1 mmol), and SCMNPs@Uridine/Zn (15 mg).

Initially, hydrazine hydrate 1 and activated ethyl acetoacetate 3 by SCMNPs@Uridine/Zn produce intermediate 11 and eliminate ethanol as a side product. In the next phase of mechanism study, Knoevenagel condensation of aldehyde 2 with barbituric acid 4 in the presence of SCMNPs@ Uridine/Zn affords intermediate 10. A subsequent Michael addition of intermediates 10 and 11 in the presence of SCMNPs@Uridine/Zn follows by intramolecular cyclization (12), dehydration and tautomerization (13) lead to the formation of product 5.
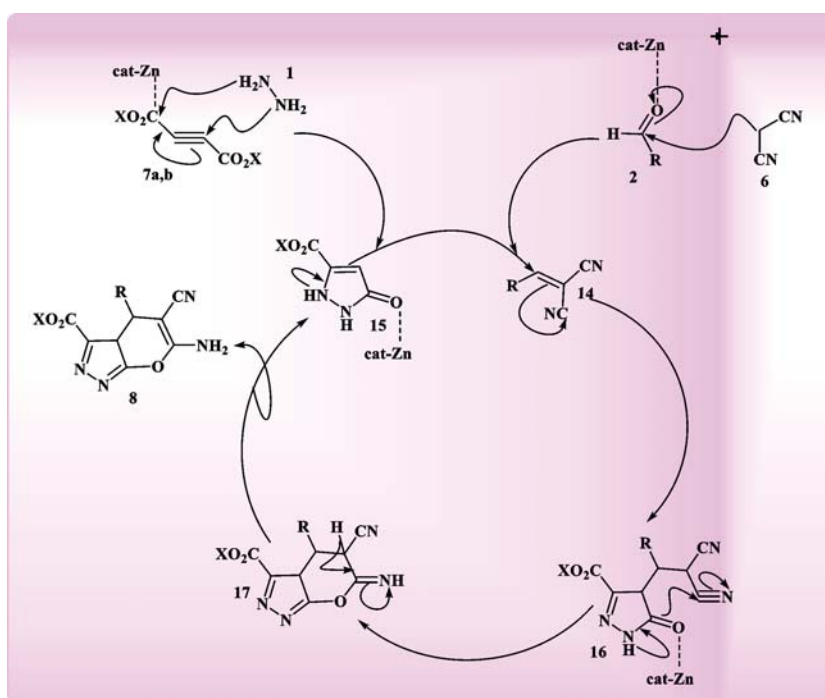
A Plausible mechanism for the synthesis of 3-methyl carboxylate substituted pyrano[2,3-c]pyrazole derivatives 8 from hydrazine hydrate, aldehyde, malononitrile, and dimethyl acetylenedicarboxylate (7a)/diethyl acetylenedicarboxylate (7b) catalyzed by SCMNPs@Uridine/Zn is shown in Scheme 4. The intermediate 15 was formed by condensation of hydrazine and dimethyl acetylenedicarboxylate (7a)/diethyl acetylenedicarboxylate (7b) in the presence of SCMNPs@Uridine/Zn. Our heterogeneous nanocatalyst played a major role in the formation of alkylidenemalononitrile 14 by the Knoevenagel con-

densation of malononitrile and aldehyde. Subsequently, intermediate 15 was reacted with alkylidenemalononitrile 14 through a Michael addition reaction to afford intermediate 16, which tolerated an intramolecular cyclization by the nucleophilic addition of the amidic oxygen to the nitrile group to produce intermediate 17. The SCMNPs@ Uridine/Zn could facilitate intermediate 17 to provide the target product 8.

The reusability of the SCMNPs@Uridine/Zn in the preparation of 3-methyl-4-(4-nitrophenyl)-4,8-dihydropyrazolo[4',3':5,6]pyrano[2,3-d]pyrimidine-5,7(1H,6H)-dione (5k) and methyl 6-amino-5-cyano-4-(4-nitrophenyl)-1,4-dihydropyrano[2,3-c]pyrazole-3-carboxylate (8f) under the optimized reaction conditions was also studied for six runs. To achieve this goal, after the completion of the reaction, the achieved solid product was dissolved in a hot ethanol. After that, the SCMNPs@Uridine/Zn was extracted using a permanent magnetic field. The separated catalyst was rinsed with deionized water, dried, and used for six runs with a negligible decrease in catalytic activity (Table 5).

Scheme 4. Plausible mechanism for synthesis of 3-methyl carboxylate substituted pyrano[2,3-c]pyrazole derivatives

Table 5. The reusability of the SCMNPs@Uridine/Zn in the preparation of 3-methyl-4-(4-nitrophenyl)-4,8-dihydropyrazolo[4',3':5,6] pyrano[2,3-d]pyrimidine-5,7(1H,6H)-dione (5k) and methyl 6-amino-5-cyano-4-(4-nitrophenyl)-1,4-dihydropyrano[2,3-c] pyrazole-3-carboxylate (8f)

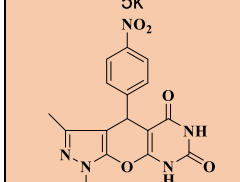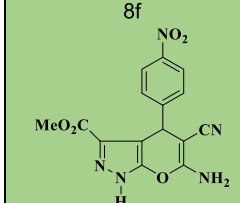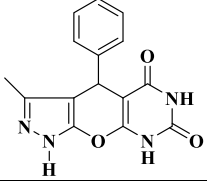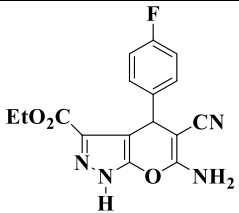|	Run	1	2	3	4	5	6
5k	Time [min]	15	15	16	17	17	18
	Yield [%]	96	96	95	94	94	93
8f	Time [min]	15	15	15	16	16	17
	Yield [%]	97	97	96	96	95	94

Table 6 illustrates the efficiency of SCMNPs@Uridine/Zn as the novel and effective magnetic nanocatalyst in the synthesis of pyrazolopyranopyrimidine and 3-methyl carboxylate substituted pyrano[2,3-*c*]pyrazole derivatives compared with several of the previously reported catalysts. It is clear that a suitable strategy in terms of product yield, reaction time, and compatibility with the environment in the presence of a low amounts of the SCMNPs@Uridine/Zn has been developed.

LITERATURE CITED

1. Hu, L., Yang, X. & Dang, S. (2011). An easily recyclable Co/SBA-15 catalyst: heterogeneous activation of peroxymonosulfate for the degradation of phenol in water. *Appl. Catal. B: Environ.* 102(1–2), 19–26. DOI:10.1016/j.apcatb.2010.11.019.

2. Yamaguchi, K. & Mizuno, N. (2002). Supported ruthenium catalyst for the heterogeneous oxidation of alcohols with molecular oxygen. *Angew. Chemie Internat. Edit.* 41(23), 4538–4542. DOI:10.1002/1521-3773(20021202)41:23<4538::AID-ANIE4538>3.0.CO;2-6.

Table 6. Comparison of the current procedure with several of the previously reported strategies for synthesizing pyrazolopyranopyrimidine and 3-methyl carboxylate substituted pyrano[2,3-*c*]pyrazole derivatives

Entry	Conditions	Temp [°C]	Time [min]	Yield [%]	Ref.
1	DABCO/H_2O	Reflux	20	99	33
2	TiO_2 NWs/H_2O-EtOH	Reflux	60	95	35
3	Oleic acid/H_2O	Reflux	12 h	82	37
4	Meglumine/H_2O	–	15	90	38
5	MNPs@DABCO$^+$Cl$^-$/Solvent-free	80	5	95	46
6	SCMNPs@Uridine/Zn /Solvent-free	70	15	97	This work
1	L-Proline/solvent-free	–	10	93	44
2	γ-Alumina/H_2O	Reflux	30	90	23
3	Amberlyst A21	–	30	90	43
4	DIPEA/EtOH	Reflux	45	93	47
5	Ba(OH)$_2$/H_2O	Reflux	1.5	93	42
6	SCMNPs@Uridine/Zn /Solvent-free	–	15	95	This work

CONCLUSION

Magnetically recoverable SCMNPs@Uridine/Zn was found to be a highly efficient and economically sustainable heterogeneous nanocatalyst for preparing a broad range of substituted tricyclic fused pyrazolopyranopyrimidine and 3-methyl carboxylate substituted pyrano[2,3-*c*]pyrazole derivatives through a one-pot four-component condensation reaction. The considerable features of this procedure are good-to-excellent product yield, short reaction time, green and mild reaction conditions, as well as the use of an easily magnetically recyclable catalyst. This procedure suggests various merits, including lower loading of the catalyst, the usage of a green catalyst, no hazardous solvent, and easy work-up. The catalyst was completely characterized using various techniques, including Fourier transform infrared spectroscopy (FT-IR), energy dispersive X-ray (EDX), thermogravimetric analysis (TGA), X-ray diffraction (XRD), and vibrating sample magnetometer (VSM).

3. Mori, K., Hara, T., Mizugaki, T., Ebitani, K. & Kaneda, K. (2004). Hydroxyapatite-supported palladium nanoclusters: a highly active heterogeneous catalyst for selective oxidation of alcohols by use of molecular oxygen. *J. Amer. Chem. Soc.* 126(34), 10657–10666. DOI:10.1021/ja0488683.

4. Mahmoudi, M., Sant, S., Wang, B., Laurent, S. & Sen, T. (2011). Superparamagnetic iron oxide nanoparticles (SPIONs): development, surface modification and applications in chemotherapy. *Adv. Drug Delivery Rev.* 63(1–2), 24–46. DOI:10.1016/j.addr.2010.05.006.

5. Lou, L., Yu, K., Zhang, Z., Huang, R., Wang, Y. & Zhu, Z. (2012). Facile methods for synthesis of core–shell structured and heterostructured Fe3O4@ Au nanocomposites. *Appl. Surf. Sci.* 258(22), 8521–8526. DOI:10.1016/j.apsusc.2012.05.031.

6. Baig, R.N. & Varma, R.S. (2013). Magnetically retrievable catalysts for organic synthesis. *Chem. Commun.* 49(8), 752–770. DOI:10.1039/C2CC35663E.

7. Rajabi, F., Karimi, N., Saidi, M.R., Primo, A., Varma, R.S. & Luque, R. (2012). Unprecedented selective oxidation of styrene derivatives using a supported iron oxide nanocatalyst in aqueous medium. *Adv. Synt. & Catal.* 354(9), 1707–1711. DOI:10.1002/adsc.201100630.

8. Kotarba, A., Bieniasz, W., Kuśtrowski, P., Stadnicka, K. & Sojka, Z. (2011). Composite ferrite catalyst for ethylbenzene dehydrogenation: Enhancement of potassium stability and catalytic performance by phase selective doping. *Appl. Catal. A: General*, 407(1–2), 100–105. DOI:10.1016/j.apcata.2011.08.029.

9. Kantam, M.L., Yadav, J., Laha, S., Srinivas, P., Sreedhar, B. & Figueras, F. (2009). Asymmetric hydrosilylation of ketones catalyzed by magnetically recoverable and reusable copper ferrite nanoparticles. *J. Org. Chem.* 74(12), 4608–4611. DOI:10.1021/jo9002823.

10. Saha, A., Leazer, J. & Varma, R.S. (2012). O-Allylation of phenols with allylic acetates in aqueous media using a magnetically separable catalytic system. *Green Chem.* 14(1), 67–71. DOI:10.1039/C1GC16174A.

11. Ismail, Z.H., Aly, G.M., El-Degwi, M.S., Heiba, H.I. & Ghorab, M.M. (2003). Synthesis and insecticidal activity of some new pyranopyrazoles, pyrazolopyranopyrimidines, and pyrazolopyranopyridines. *Egypt. J. Biotechnol.* 13, 73–82. DOI :10.1080/00397911.2015.1129668.

12. Nasr, M.N. & Gineinah, M.M. (2002). Pyrido [2, 3-d] pyrimidines and Pyrimido [5′, 4′: 5, 6] pyrido [2, 3-d] pyrimidines as New Antiviral Agents: Synthesis and Biological Activity. Archiv der Pharmazie: *An Internat. J. Pharmac. Med. Chem.* 335(6), 289–295. DOI:10.1002/1521-4184(200208)335:6<289::AID-ARDP289>3.0.CO;2-Z.

13. Abdelrazek, F.M., Metz, P., Metwally, N.H. & El-Mahrouky, S.F. (2006). Synthesis and Molluscicidal Activity of New Cinnoline and Pyrano [2, 3-c] pyrazole Derivatives. Archiv der Pharmazie: *An Internat. J. Pharmac. Med. Chem.* 339(8), 456–460. DOI:10.1002/ardp.200600057.

14. Abdelrazek, F.M., Metz, P., Kataeva, O., Jaeger, A., & El-Mahrouky, S.F. (2007). Synthesis and molluscicidal activity of new chromene and pyrano [2, 3-c] pyrazole derivatives. Archiv der Pharmazie: *An Internat. J. Pharmac. Med. Chem.* 340(10), 543–548. DOI:10.1002/ardp.200700157.

15. Feurer, A., Luithle, J., Wirtz, S., Koenig, G., Stasch, J., Stahl, E. & Lang, D. (2004). PCT Int. Appl. WO 2004009589 (Bayer Healthcare AG, Germany). *Chem. Abstr. Vol.* 140, p. 146157.

16. Kuo, S.C., Huang, L.J. & Nakamura, H. (1984). Studies on heterocyclic compounds. 6. Synthesis and analgesic and antiinflammatory activities of 3, 4-dimethylpyrano [2, 3-c] pyrazol-6-one derivatives. *J. Med. Chem.* 27(4), 539–544. DOI:10.1021/jm00370a020.

17. Zaki, M.E., Soliman, H.A., Hiekal, O.A. & Rashad, A.E. (2006). Zeitschrift fur Naturforschung. *C. J. Biosci.* 61, 1.

18. Wang, J.L., Liu, D., Zhang, Z.J., Shan, S., Han, X., Srinivasula, S.M. & Huang, Z. (2000). Structure-based discovery of an organic compound that binds Bcl-2 protein and induces apoptosis of tumor cells. Proceed. National Acad. Sci. 97(13), 7124–7129. DOI:10.1073/pnas.97.13.7124.

19. Junek, H. & Aigner, H. (1973). Synthesen mit Nitrilen, XXXV. Reaktionen von tetracyanäthylen mit heterocyclen. *Chem. Berichte*, 106(3), 914–921. DOI:10.1002/cber.19731060323.

20. Vasuki, G. & Kumaravel, K. (2008). Rapid four-component reactions in water: synthesis of pyranopyrazoles. *Tetrahedron Letters*, 49(39), 5636–5638. DOI:10.1016/j.tetlet.2008.07.055.

21. Gogoi, S. & Zhao, C.G. (2009). Organocatalyzed enantioselective synthesis of 6-amino-5-cyanodihydropyrano [2, 3-c] pyrazoles. *Tetrahedron Letters*, 50(19), 2252–2255. DOI:10.1016/j.tetlet.2009.02.210.

22. Mecadon, H., Rohman, M.R., Kharbangar, I., Laloo, B.M., Kharkongor, I., Rajbangshi, M. & Myrboh, B. (2011). L-Proline as an efficient catalyst for the multi-component synthesis of 6-amino-4-alkyl/aryl-3-methyl-2, 4-dihydropyrano [2, 3-c] pyrazole-5-carbonitriles in water. *Tetrahedron Letters*, 52(25), 3228–3231. DOI:10.1016/j.tetlet.2011.04.048.

23. Mecadon, H., Rohman, M.R., Rajbangshi, M. & Myrboh, B. (2011). γ-Alumina as a recyclable catalyst for the four-component synthesis of 6-amino-4-alkyl/aryl-3-methyl-2, 4-dihydropyrano [2, 3-c] pyrazole-5-carbonitriles in aqueous medium. *Tetrahedron Letters*, 52(19), 2523–2525. DOI:10.1016/j.tetlet.2011.03.036.

24. Reddy, M.M., Jayashankara, V.P. & Pasha, M.A. (2010). Glycine-catalyzed efficient synthesis of pyranopyrazoles via one-pot multicomponent reaction. Synthetic Communications®, 40(19), 2930–2934. DOI:10.1080/00397910903340686.

25. Siddekha, A., Nizam, A. & Pasha, M.A. (2011). An efficient and simple approach for the synthesis of pyranopyrazoles using imidazole (catalytic) in aqueous medium, and the vibrational spectroscopic studies on 6-amino-4-(4′-methoxyphenyl)-5-cyano-3-methyl-1-phenyl-1, 4-dihydropyrano [2, 3-c] pyrazole using density functional theory. *Spectrochim. Acta Part A: Molec. Biomol. Spectrosc.* 81(1), 431–440. DOI:10.1016/j.saa.2011.06.033.

26. Mohamed, N.R., Khaireldin, N.Y., Fahmyb, A.F. & El-Sayeda, A.A.F. (2010). Facile synthesis of fused nitrogen containing heterocycles as anticancer agents. *Der. Pharm. Chem.* 2, 400–417.

27. Prasad, Y.R., Rao, A.L., Prasoona, L., Murali, K. & Kumar, P.R. (2005). Synthesis and antidepressant activity of some 1, 3, 5-triphenyl-2-pyrazolines and 3-(2″-hydroxy naphthalen-1″-yl)-1, 5-diphenyl-2-pyrazolines. *Bioorg. & Med. Chem. Letters*, 15(22), 5030–5034. DOI:10.1016/j.bmcl.2005.08.040.

28. Ahluwalia, V.K., Dahiya, A. & Garg, V.K. (1997). Reaction of 5-Amino-4-formyl-3-methyl (or phenyl)-1-phenyl-1H-pyrazoles with Active Methylene Compounds: Synthesis of Fused Heterocyclic Rings. ChemInform, 28(40), no-no.

29. Furuya, S. & Ohtaki, T. (1994). Pyrido [2, 3-d] pyrimidines and their uses as anatagonists. *Eur. Pat. Appl. Ep.* 608565.

30. Valderrama, J.A. (2008). Synletters (2006) 2777e2780;(b) JA Valderrama, P. Colonelli, D. Vásquez, MF González, JA Rodríguez, C. Theoduloz. *Bioorg. Med. Chem.* 16, 10172–10181. DOI:10.1016/j.bmc.2008.10.064.

31. Bagley, M.C., Hughes, D.D., Lubinu, M.C., Merritt, E.A., Taylor, P.H. & Tomkinson, N.C. (2004). Microwave-assisted synthesis of pyrimidine libraries. *QSAR & Combinat. Sci.* 23(10), 859–867. DOI:10.1002/qsar.200420044.

32. Kamdar, N.R., Haveliwala, D.D., Mistry, P.T., & Patel, S.K. (2010). Design, synthesis and in vitro evaluation of antitubercular and antimicrobial activity of some novel pyranopyrimidines. *Europ. J. Med. Chem.* 45(11), 5056–5063. DOI:10.1016/j.ejmech.2010.08.014.

33. Heravi, M.M., Mousavizadeh, F., Ghobadi, N., & Tajbakhsh, M. (2014). A green and convenient protocol for the synthesis of novel pyrazolopyranopyrimidines via a one-pot, four-component reaction in water. *Tetrahedron Letters*, 55(6), 1226–1228. DOI:10.1016/j.tetlet.2014.01.004.

34. Khodabakhshi, S., Rashidi, A., Tavakoli, Z., Baghernejad, M., & Yadegari, A. (2016). The first catalytic application of oxidized carbon nanotubes in a four-component synthesis of fused heterocycles. *Monatshefte für Chemie-Chemical Monthly*, 147(4), 791–795. DOI:10.1007/s00706-015-1532-6.

35. Dastkhoon, S., Tavakoli, Z., Khodabakhshi, S., Baghernejad, M. & Abbasabadi, M.K. (2015). Nanocatalytic one-pot, four-component synthesis of some new triheterocyclic compounds consisting of pyrazole, pyran, and pyrimidinone rings. *J. Chem.* 39(9), 7268–7271. DOI:10.1039/C5NJ01046B.

36. Wang, S., Izquierdo, J., Rodríguez-Escrich, C. & Pericàs, M.A. (2017). Asymmetric [4+ 2] Annulation Reactions Catalyzed by a Robust, Immobilized Isothiourea. *ACS Catal.* 7(4), 2780–2785. DOI:10.1021/acscatal.7b00360.

37. Ganesan, A., Kothandapani, J. & Subramaniapillai, S.G. (2016). Extending the scope of oleic acid catalysis in diversity-oriented synthesis of chromene and pyrimidine based scaffolds. *RSC Adv.* 6(25), 20582–20587. DOI:10.1039/C6RA02507B.

38. Li, X.T., Zhao, A.D., Mo, L.P. & Zhang, Z.H. (2014). Meglumine catalyzed expeditious four-component domino protocol for synthesis of pyrazolopyranopyrimidines in aqueous medium. *RSC Adv.* 4(93), 51580–51588. DOI:10.1039/C4RA08689A.

39. Safaei-Ghomia, J., Asgari-Kheirabadia, M., Shahbazi-Alavia, H. & Ziaratib, A. (2016). Synthesis of methyl 6-amino-

5-cyano-4-aryl-2, 4-dihydropyrano [2, 3-c] pyrazole-3-carboxylates using nano-ZnZr4 (PO4) 6 as an efficient catalyst. *Iranian J. Catal*. 6(4), 319–324.

40. Safaei-Ghomi, J., Asgari-Kheirabadi, M., & Shahbazi-Alavi, H. (2016). Environmentally benign synthesis of methyl 6-amino-5-cyano-4-aryl-2, 4-dihydropyrano [2, 3-c] pyrazole-3-carboxylates using CeO2 nanoparticles as a reusable and robust catalyst. *Zeitschrift für Naturforschung B,* 71(11), 1135–1140. DOI:10.1515/znb-2016-0119.

41. Zonouz, A.M., Eskandari, I., & Khavasi, H.R. (2012). A green and convenient approach for the synthesis of methyl 6-amino-5-cyano-4-aryl-2, 4-dihydropyrano [2, 3-c] pyrazole-3-carboxylates via a one-pot, multi-component reaction in water. *Tetrahedron Letters*, 53(41), 5519–5522. DOI:10.1016/j.tetlet.2012.08.010.

42. Azzam, S.H.S. & Pasha, M.A. (2012). Simple and efficient protocol for the synthesis of novel dihydro-1H-pyrano [2, 3-c] pyrazol-6-ones via a one-pot four-component reaction. *Tetrahedron Letters*, 53(50), 6834–6837. DOI:10.1016/j.tetlet.2012.10.025.

43. Bihani, M., Bora, P.P., Bez, G., & Askari, H. (2013). Amberlyst A21 catalyzed chromatography-free method for multicomponent synthesis of dihydropyrano [2, 3-c] pyrazoles in ethanol. *ACS Sustain. Chem. & Engin.* 1(4), 440–447. DOI:10.1021/sc300173z.

44. Ambethkar, S., Padmini, V. & Bhuvanesh, N. (2015). A green and efficient protocol for the synthesis of dihydropyrano [2, 3-c] pyrazole derivatives via a one-pot, four component reaction by grinding method. *J. Adv. Res.* 6(6), 975–985. DOI:10.1016/j.jare.2014.11.011.

45. Bhaskaruni, S.V., Maddila, S., van Zyl, W.E., & Jonnalagadda, S.B. (2018). An efficient and green approach for the synthesis of 2, 4-dihydropyrano [2, 3-c] pyrazole-3-carboxylates using Bi 2 O 3/ZrO 2 as a reusable catalyst. *RSC Adv.* 8(29), 16336–16343. DOI:10.1039/C8RA01994K.

46. Rigi, F. & Shaterian, H.R. (2016). Magnetic Nanoparticle Supported Ionic Liquid Assisted Green Synthesis of Pyrazolopyranopyrimidines and 1, 6-diamino-2-oxo-1, 2, 3, 4-tetrahydropyridine-3, 5-dicarbonitriles. *J. Chin. Chem. Soc.* 63(7), 557–561. DOI:10.1002/jccs.201500407.

47. Zolfigol, M.A., Tavasoli, M., Moosavi-Zare, A.R., Moosavi, P., Kruger, H.G., Shiri, M. & Khakyzadeh, V. (2013). Synthesis of pyranopyrazoles using isonicotinic acid as a dual and biological organocatalyst. *RSC Adv*. 3(48), 25681–25685. DOI:10.1039/C3RA45289A.